

1 Increasingly powerful tornadoes in the United States

2 James B. Elsner¹, Tyler Fricker¹, Zoe Schroder¹

3 ¹Department of Geography, Florida State University, Tallahassee, FL 32306, USA

4 **Key Points:**

- 5 • Tornadoes in the U.S. appear to be getting more powerful
- 6 • The trend is independent of occurrence time and changes to the damage scale
- 7 • Part of the trend is linked to increases in convective inhibition and to CAPE
- 8 conditional on increasing shear.

Corresponding author: James B. Elsner, jelsner@fsu.edu

Abstract

Storm reports show an upward trend in the power of tornadoes from longer and wider paths and higher damage ratings. Quantifying the magnitude of the increase is difficult given diurnal and seasonal influences on tornadoes embedded within natural variations and made worse by changes for rating damage. Here the authors solve this problem by fitting a statistical model to a metric of power during the period 1994–2016. They find an increase of 5.5% [(4.6, 6.5%), 95% CI] per year in tornado power controlling for the diurnal cycle, seasonality, natural climate variability, and the switch to a new damage scale. A portion of the trend is attributed to long-term changes in convective storm environments involving dynamic and thermodynamic variables and their interactions. Increasing tornado power is occurring in environments where the effect of convective available potential energy is enhanced by increasing vertical wind shear.

1 Introduction

Tornadoes are nature’s most violent storms with winds that can exceed 120 m s^{-1} . A mobile Doppler radar estimated a near-ground-level wind speed of 135 m s^{-1} in the Bridge Creek-Moore, Oklahoma tornado of May 3, 1999. How global warming will affect tornadoes remains an open question. It has been argued that because of data inadequacy and limited physical understanding of the processes that cause tornadoes it is difficult to find trends related to climate change (Kunkel et al., 2013). However these arguments are based on studies that are at least five years old, focus exclusively on tornado occurrences, and use methods that lack ways to include intervening factors at multiple levels (e.g., hourly and seasonal). Here we focus on tornado power and use a hierarchical statistical model that controls for the known behavior of tornado activity.

We note that while the annual number of strong and violent tornadoes (EF2 or worse) has remained relatively consistent from year to year, the number of days with many tornadoes is on the rise (Brooks, Carbin, & Marsh, 2014; Elsner, Elsner, & Jagger, 2015; Tippett, Lepore, & Cohen, 2016; Tippett, Sobel, Camargo, & Allen, 2014). An increase in the number of big tornado days implies a larger threat of damaging tornadoes (Elsner, Jagger, Widen, & Chavas, 2014) with the percentage of violent tornadoes (EF4 or worse) increasing with increasing outbreak size. Less than 4% of tornadoes occurring on days with between 16 and 31 tornadoes are rated EF3 or higher while more than 8% of tornadoes occurring on days with more than 63 tornadoes are rated similarly (Table 1). Increases occur for the percentage of violent (EF4 and EF5) tornadoes as well. This leads us to hypothesize that tornadoes have become more powerful.

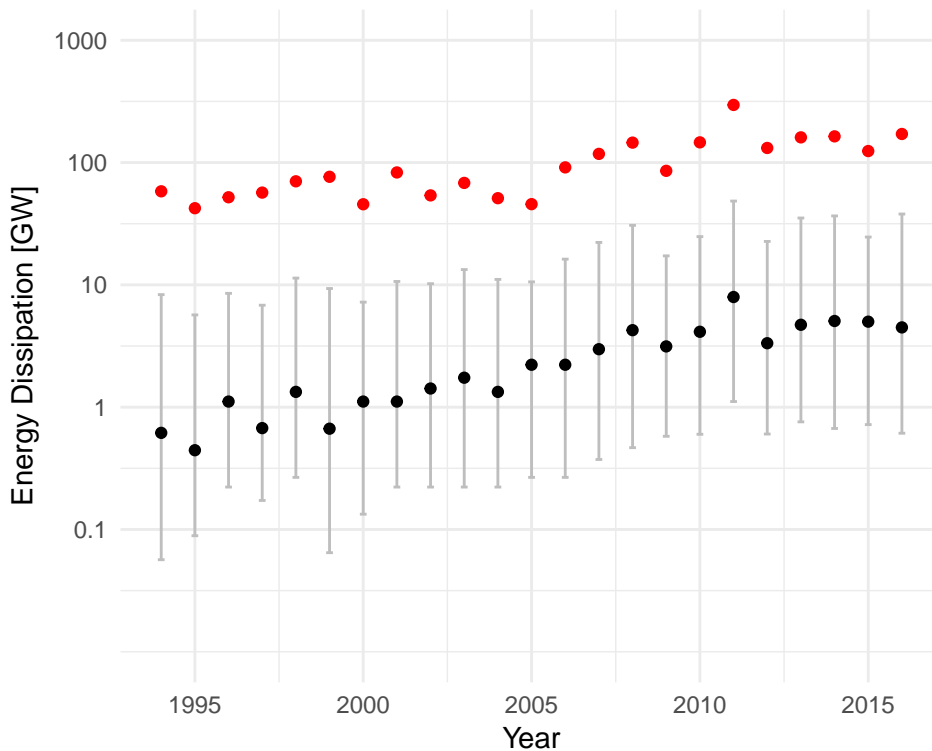
Table 1. Tornado statistics by tornado-day size. Numbers are based on all tornado reports over the period 1994–2016. Data are from the Storm Prediction Center.

Tornado Day Size (No. Tor.)	Number of Cases	Total Number of Tor.	% Tor. Rated Intense (EF3+)	% Tor. Rated Violent (EF4+)
1	1088	1088	0.37	0.00
2-3	1068	2581	0.39	0.00
4-7	874	4521	0.82	0.09
8-15	644	6921	1.99	0.38
16-31	295	6466	3.34	0.57
32-63	103	4355	5.49	1.08
>63	25	2018	8.18	2.23

45 2 Results

46 Tornado power is metered by the energy dissipated near the ground (Fricker,
 47 Elsner, & Jagger, 2017). On average the longest lasting tornadoes generate the most
 48 extreme wind speeds (Brooks, 2004; Elsner, Jagger, & Elsner, 2014; Fricker & Elsner,
 49 2015). And indeed damage paths are getting longer (see Appendix Fig. A1). Multi-
 50 plying path area, air density, and wind speed gives an estimate of the total energy
 51 dissipated by a tornado (Fricker et al., 2017) (See §Methods). For the set of 27,950 tor-
 52 nadoes during the period 1994–2016, the median energy dissipation is 2.22 gigawatts
 53 (GW) with an inter-quartile range between .27 and 17 GW. Tornado power is highly
 54 correlated ($r > .9$) with the destructive potential index developed at the U.S. Storm
 55 Prediction Center (SPC) (Fricker & Elsner, 2015) and with the number of casualties
 56 when people are present (Fricker et al., 2017). The Tallulah-Yazoo City-Durant tor-
 57 nado (Louisiana and Mississippi) of 24 April 2010 that killed ten and injured 146 had
 58 an estimated power of 66,200 GW. Annual statistics of tornado power show clear up-
 59 ward trends with the median, quartiles, and 90th percentile all on the rise over the
 60 period 1994–2016 (Fig. 1).

Figure 1. Annual energy dissipation by year. The black dot is the median and the red dot is the 90th percentile value each year. The vertical bar extends from the lower to upper quartile numbers.

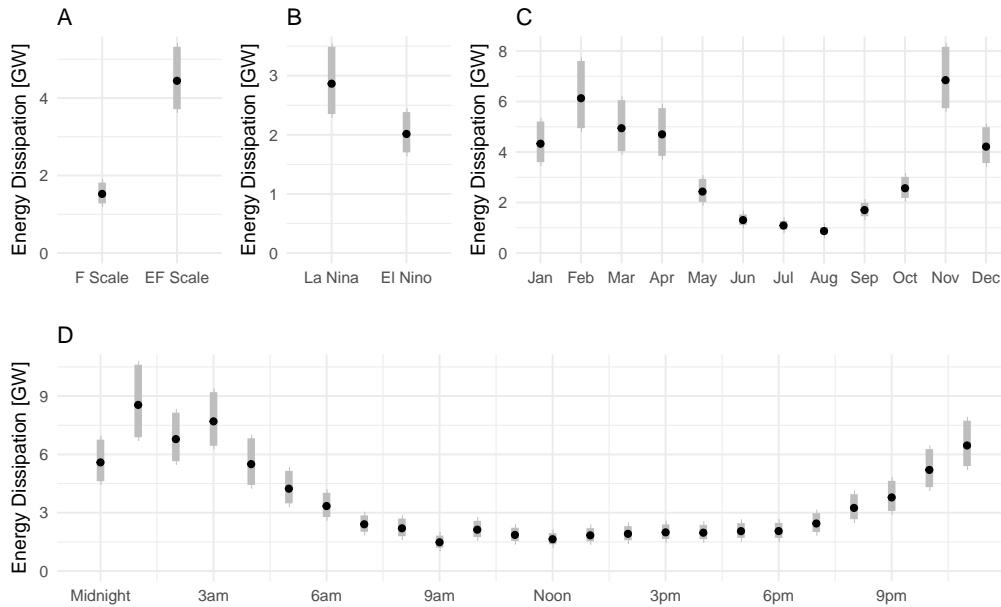


61 The observed increase in power might be the result of shifts in when and where
 62 tornadoes occur (Agee, Larson, Childs, & Marmo, 2016). Also, at least a portion of
 63 the rise is due to a change in the procedures to rate the damage left behind. The EF
 64 damage rating scale was revised from the original F scale (and was put into operational
 65 use in 2007) with better standards for determining what was previously subjective
 66 including additional structures and vegetation, expanded degrees of damage, and a
 67 better accounting of construction quality. Figure 2 shows tornado power grouped by

68 the change in the EF rating scale, El Niño/La Niña, month of occurrence (genesis),
 69 and by time of day (in hours). Mean energy dissipation is relatively higher at night,
 70 during La Niña, in the cooler months, and after the implementation of the EF rating
 71 procedure.

72 To test the hypothesis of an upward trend, after accounting for these known
 73 influences, we fit a hierarchical regression model to the per-tornado power using all
 74 available tornado reports over the period 1994–2016. The model has a log-normal
 75 distribution for the likelihood on the per-tornado power where a lower bound is set at
 76 444 kW; a value just below the least powerful tornado in the record. Fixed effects in the
 77 model include the bivariate index for ENSO and a variable to mark the year when the
 78 switch to the new damage rating procedures were put in place (2007). Random effects
 79 include month and hour to capture the cyclic change in energy at these respective time
 80 scales. A term indexing the year of occurrence is included as a fixed effect to test our
 81 hypothesis and to quantify the residual trend per annum (see §Methods Summary).

Figure 2. Energy dissipation grouped by EF change, ENSO, month, and hour. The dot is the geometric mean for each subgroup and the gray bars extend one standard deviation from the mean.



82 As expected the model shows the cycle of alternating ocean-atmosphere conditions
 83 in the equatorial Pacific, known as ENSO, is an important and significant
 84 influence on tornado power with a regression coefficient expressed as a multiplicative
 85 decrease of .93 [(.90, .96), 95% CI] for every one standard deviation increase (going
 86 from La Niña to El Niño) in the bivariate ENSO index (exponentiating the coefficient
 87 in Table 2). This is consistent with the fact that under La Niña conditions (especially
 88 during winter) amplified upper-air troughs move across North America with warmer
 89 than normal temperatures in the Southeast and cooler than normal temperatures in
 90 the Northwest, which sets the stage for severe weather outbreaks that are intensified
 91 by a strong jetstream (Allen, Tippett, & Sobel, 2015; Cook, Leslie, Parsons, & Schaefer,
 92 2017; Cook & Schaefer, 2008). The model also shows that the procedures put in
 93 place following the adoption of the EF damage rating scale results in an increase in
 94 power by a factor of 1.41 [(1.24, 1.59), 95% CI]. This increase is expected given the

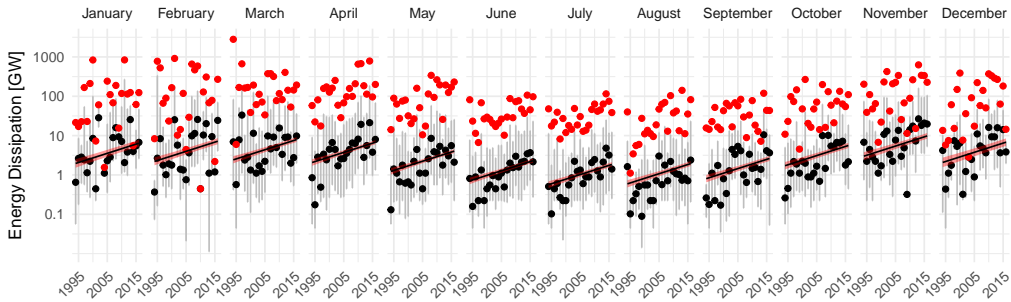
95 improvements after adoption in damage surveys including more precise and inclusive
 96 damage indicators.

Table 2. Fixed effects. Estimated coefficients on the fixed effects terms in the model. The Error is one standard deviation. The lower and upper 95% credible intervals are given.

	Estimate	Error	l-95% CI	u-95% CI
α	21.298	0.023	21.253	21.344
β_{ENSO}	-0.068	0.016	-0.101	-0.036
$\beta_{\text{EF?}}$	0.341	0.063	0.217	0.462
β_{Year}	0.054	0.005	0.045	0.063

97 Most importantly the model shows a significant upward trend in tornado power
 98 at a rate of 5.5% [(4.6, 6.5%), 95% CI] per year. The magnitude of the increase depends
 99 on the data and the model that controls for diurnal and seasonal variability, the ENSO
 100 cycle, and implementation of the EF rating scale. The model quantifies the increasing
 101 ferocity of tornadoes independent of the other factors considered and lends support
 102 to our hypothesis that as tornado-days become larger the tornadoes themselves are
 103 becoming more powerful. The base rate from which the upward trend depends on the
 104 time of the year through the random-effect term, but the monthly trends appear to
 105 track the data well (Fig. 3).

Figure 3. Upward trends in tornado power by month. The black dot is the median and the red dot is the 90th percentile value each year. The vertical bar extends from the lower to upper quartile numbers. The black line is the modeled trend with a 95% CI band shown in red shading.



106 **3 Discussion**

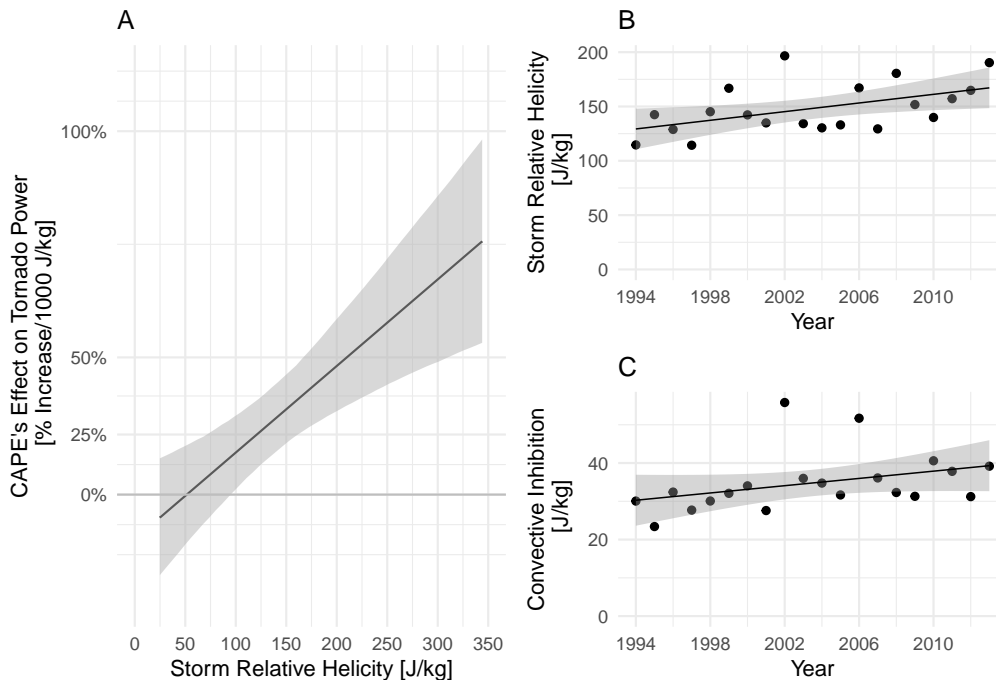
107 The study is retrospective but our hierarchical modeling strategy can help un-
 108 cover clues about what might be happening as the earth warms. We conjecture
 109 that at least a portion of the upward trend in tornado power is related to long-term
 110 changes in regional environments associated with severe thunderstorms. Modeling
 111 studies project increases in convective available energy (CAPE) with a warmer cli-
 112 mate (DelGenio, Yao, & Jonas, 2007; Diffenbaugh, Scherer, & Trapp, 2013; Trapp,
 113 Diffenbaugh, & Gluhovsky, 2009), and we previously hypothesized that climate change
 114 and increases in CAPE could be leading to more active areas of severe convection on
 115 days with tornadoes (Elsner, Jagger, & Elsner, 2014). Increases in CAPE with global

116 warming are documented in both climate models (Sobel & Camargo, 2011) and cloud-
 117 system-resolving models (Romps, 2011), and these increases have theoretical support
 118 (Seeley & Romps, 2015; Singh & O’Gorman, 2013).

119 .

120 Here we examine how regional environmental factors including CAPE, convective
 121 inhibition (CIN), and storm relative helicity (SRH) are related to the trend in tornado
 122 power. We use gridded reanalysis data at 1800 UTC on (outbreak) days with at least
 123 ten tornadoes (there are 748 such days in the period January 1994 through September
 124 2014). We spatially average values for each of the three environmental variables sepa-
 125 rately over all grids within the domain defined by the tornado genesis locations for that
 126 day. Averages over all outbreak days by year show upward trends in SRH (Tippett et
 127 al., 2016) and SRH (Fig. 4[B & C]). We include the environmental variables in models
 128 for average tornado power (averaged over all tornadoes in the outbreak and scaled by
 129 the area of the domain) and find the best model when CAPE and SRH are used as an
 130 interaction term. In other words, the model indicates that CAPE’s effect on tornado
 131 power is significantly enhanced with increasing SRH (Fig. 4[A]). For example, with
 132 average SRH values at 100 J/kg tornado power increases by 18% per 1000 J/kg of
 133 CAPE but with average SRH values of 250 J/kg power increases by 55% for the same
 134 1000 J/kg of CAPE. Importantly the magnitude of the trend in a model that includes
 135 the environmental variables is 24% lower compared with the magnitude of the trend in
 136 a model that excludes the variables. Thus we conclude that increasing tornado power
 137 is occurring in environments with increasing CIN and in environments where the effect
 138 of CAPE is being enhanced by increasing SRH.

Figure 4. Upward trends in storm relative helicity (SRH), convective inhibition (CIN), and the conditional effect of convective available potential energy (CAPE). The sloping black lines denote point estimates of the trends and the gray ribbons indicate the 95% uncertainty bound around the point estimates.



139 In summary, we identified an upward trend in tornado power after accounting
 140 for known factors and then demonstrated that a portion of the trend is statistically
 141 related to CAPE conditional on SRH. More definitive answers to important questions
 142 concerning climate change and tornadoes will need to wait for a better theoretical
 143 understanding of tornado processes. But the large number tornadoes that occur each
 144 year provides a generous sample that allows researchers to use hierarchical model to
 145 separate potential climate-change signals from noise.

146 4 Methods

147 4.1 Energy dissipation (power)

Energy dissipation (power) for each tornado is computed as:

$$E = A_p \rho \sum_{j=0}^5 w_j v_j^3, \quad (1)$$

148 where the summation is over the six possible EF ratings (0, 1, 2, 3, 4 and 5), A_p is
 149 the area of the tornado's path [units of square meters], ρ is air density [1 kg m^{-3}],
 150 v_j is the midpoint wind speed [m s^{-1}] for each damage rating (EF scale) j , w_j is the
 151 corresponding fraction of path area by damage rating, and 5 is the maximum damage
 152 rating. Path area is the product of path width and path length. Path length is known
 153 to a relatively high degree of accuracy (Doswell, Edwards, Thompson, Hart, & Crosbie,
 154 2006). Multiplying the units from the individual terms results in E being measured
 155 in a unit of power [$\text{kg m}^2 \text{ s}^{-3} = \text{Joule/s} = \text{Watt (W)}$]. Path length and width and
 156 maximum EF rating are listed in the Storm Prediction Center's tornado database.

157 The database is compiled from the National Weather Service's (NWS) *Storm*
 158 *Data*, and includes all known tornadoes dating back to 1950. Here we focus on the
 159 available recent period of this record from 1994–2016. The fraction of path area is that
 160 recommended by the U.S. Nuclear Regulatory Commission (Fricker & Elsner, 2015),
 161 which combines a Rankine vortex with empirical estimates derived from detailed storm
 162 surveys (Ramsdell & Rishel, 2007). Threshold wind speeds for the EF ratings are a
 163 three second gust. With no upper bound on the EF5 wind speeds, the midpoint wind
 164 speed is set at 97 m s^{-1} (7.5 m s^{-1} above the threshold wind speed consistent with
 165 the EF4 midpoint speed relative to its threshold). Tornado energy is highly correlated
 166 with the destructive potential index (Thompson & Vescio, 1998). Additional details
 167 and justification for energy dissipation as a valid measure of tornado power are given
 in Fricker et al. (2017). Tornado power by EF rating is given in Table 3.

Table 3. Tornado power by EF rating. Numbers are in gigawatts (GW) and are based on the 27,950 tornadoes over the period 1994–2016.

(E)F Rating	n	Median	Total	Arithmetic Mean	Geometric Mean
0	17182	0.5	73329.6	4.3	0.6
1	7735	12.5	364162.5	47.1	10.8
2	2224	91.4	609230.8	273.9	77.5
3	650	615.7	827474.3	1273.0	495.4
4	145	1631.0	511177.8	3525.4	1427.6
5	14	6458.5	130239.0	9302.8	5622.7

169

4.2 Statistical models

For each tornado a log-normal distribution is assumed for its power with a lower bound set to 444 kW. The geometric means of the distributions are logically related to the fixed effects and their coefficients (β 's) including year of occurrence, the bivariate ENSO index, and an indicator variable to mark the year when the switch to the new damage rating procedures were put in place. Variations in power by month and hour are modeled as random intercept effects so the corresponding coefficients are vectors of length 12 and 24, respectively. Mathematically the regression model is expressed as:

$$\ln(E|E > 444000) = \alpha + \beta_{\text{Year}}\text{Year} + \beta_{\text{ENSO}}\text{ENSO} + \beta_{\text{EF?}}\text{EF?} + \beta_{\text{Month}}(1|\text{Month}) + \beta_{\text{Hour}}(1|\text{Hour})$$

170 To examine the influence environmental variables including CAPE, CIN, and
 171 SRH have on reducing the upward trend, a similar regression model is fit to power per
 172 unit area averaged over all tornadoes on a day with at least ten tornadoes. A model
 173 using outbreak-level data (rather than tornado-level data) is needed because the scale
 174 of individual tornadoes is much smaller than the scale at which the environmental
 175 variables are resolved. Here values for the environmental variables on a regular grid
 176 are averaged over a convex polygon domain enclosing all the tornado genesis locations
 177 for that day. The best model (lowest Akaike information criterion (AIC) value) includes
 178 CIN and an interaction between CAPE and SRH.

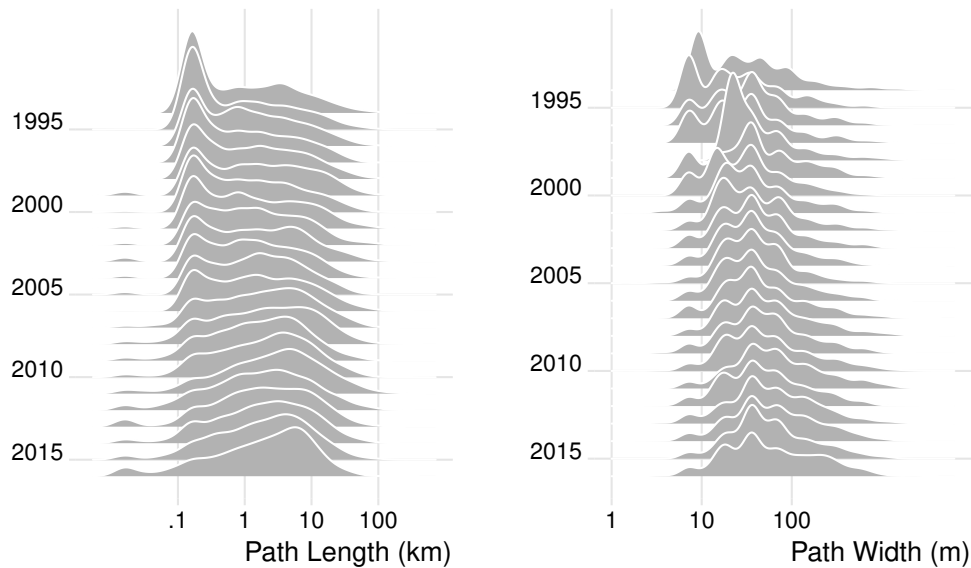
179

4.3 Code and data

180 Analysis and modeling are performed using the software environment R ([http://](http://www.r-project.org)
 181 www.r-project.org). Models are fit using maximum likelihood procedures with func-
 182 tions in the **lme4** package Bates, Mächler, Bolker, and Walker (2015) and using
 183 Bayesian simulations in the Stan computational framework (<http://mc-stan.org/>)
 184 accessed with the **brms** package Bürkner (2017). To improve convergence and guard
 185 against over-fitting with the Bayesian procedures, we specified mildly informative con-
 186 servative priors. The codes and data to reproduce the results from this study are
 187 available here <https://github.com/jelsner/tor-pwr-up> and here [https://github](https://github.com/jelsner/get-NARR)
 188 [.com/jelsner/get-NARR](https://github.com/jelsner/get-NARR).

A Distributions of path length and path width by year

Figure A1. Distributions of path length and path width by year. Path widths narrower than one meter are not plotted.



Acknowledgments

The code and data to reproduce the results from this study are available from <https://github.com/jelsner/tor-pwr-up> and <https://github.com/jelsner/get-NARR>.

References

- Agee, E., Larson, J., Childs, S., & Marmo, A. (2016, 05). Spatial redistribution of USA tornado activity between 1954 and 2013. *Journal of Applied Meteorology and Climatology*, *55*, 1681-1697.
- Allen, J. T., Tippett, M. K., & Sobel, A. H. (2015). Influence of the El Niño/Southern Oscillation on tornado and hail frequency in the United States. *Nature Geosciences*, *8*, 278-283.
- Bates, D., Mächler, M., Bolker, B., & Walker, S. (2015). Fitting linear mixed-effects models using lme4. *Journal of Statistical Software*, *67*(1), 1-48. doi: 10.18637/jss.v067.i01
- Brooks, H. E. (2004). On the relationship of tornado path length and width to intensity. *Weather and Forecasting*, *19*, 310-319.
- Brooks, H. E., Carbin, G. W., & Marsh, P. T. (2014). Increased variability of tornado occurrence in the united states. *Science*, *346*(6207), 349-352. Retrieved from <http://science.sciencemag.org/content/346/6207/349> doi: 10.1126/science.1257460
- Bürkner, P.-C. (2017). brms: An R package for bayesian multilevel models using Stan. *Journal of Statistical Software*, *80*(1), 1-28. doi: 10.18637/jss.v080.i01
- Cook, A. R., Leslie, L. M., Parsons, D. B., & Schaefer, J. T. (2017, sep). The impact of el niño-southern oscillation (ENSO) on winter and early spring u.s. tornado outbreaks. *Journal of Applied Meteorology and Climatology*, *56*(9), 2455-2478. Retrieved from <https://doi.org/10.1175/jamc-d-16-0249.1> doi: 10.1175/jamc-d-16-0249.1

- 216 Cook, A. R., & Schaefer, J. T. (2008). The relation of El Niño-Southern Oscilla-
 217 tion (ENSO) to winter tornado outbreaks. *Monthly Weather Review*, *136*,
 218 3121-3137.
- 219 DelGenio, A. D., Yao, M.-S., & Jonas, J. (2007, aug). Will moist convection be
 220 stronger in a warmer climate? *Geophysical Research Letters*, *34*(16). Retrieved
 221 from <https://doi.org/10.1029/2007gl030525> doi: 10.1029/2007gl030525
- 222 Diffenbaugh, N. S., Scherer, M., & Trapp, R. J. (2013). Robust increases in se-
 223 vere thunderstorm environments in response to greenhouse forcing. *Pro-
 224 ceedings of the National Academy of Sciences*, *110*, 16361-16366. doi:
 225 10.1073/pnas.1307758110
- 226 Doswell, C. A., Edwards, R., Thompson, R. L., Hart, J. A., & Crosbie, K. C. (2006,
 227 dec). A simple and flexible method for ranking severe weather events. *Weather
 228 and Forecasting*, *21*(6), 939–951. Retrieved from [https://doi.org/10.1175/
 229 waf959.1](https://doi.org/10.1175/waf959.1) doi: 10.1175/waf959.1
- 230 Elsner, J. B., Elsner, S. C., & Jagger, T. H. (2015). The increasing efficiency of tor-
 231 nado days in the United States. *Climate Dynamics*, *45*(3-4), 651–659.
- 232 Elsner, J. B., Jagger, T. H., & Elsner, I. J. (2014). Tornado intensity estimated from
 233 damage path dimensions. *PLoS ONE*, *9* (9), e107571.
- 234 Elsner, J. B., Jagger, T. H., Widen, H. M., & Chavas, D. R. (2014). Daily tornado
 235 frequency distributions in the United States. *Environmental Research Letters*,
 236 *9*(2), 024018.
- 237 Fricker, T., & Elsner, J. B. (2015). Kinetic energy of tornadoes in the United States.
 238 *PLoS ONE*, *10*, e0131090. doi: 10.1371/journal.pone.0131090
- 239 Fricker, T., Elsner, J. B., & Jagger, T. H. (2017). Population and energy elasticity of
 240 tornado casualties. *Geophysical Research Letters*, *44*, 3941-3949. doi: 10.1002/
 241 2017GL073093
- 242 Kunkel, K. E., Karl, T. R., Brooks, H., Kossin, J., Lawrimore, J. H., Arndt, D.,
 243 ... Wuebbles, D. (2013, apr). Monitoring and understanding trends in
 244 extreme storms: State of knowledge. *Bulletin of the American Meteorolog-
 245 ical Society*, *94*(4), 499–514. Retrieved from [https://doi.org/10.1175/
 246 bams-d-11-00262.1](https://doi.org/10.1175/bams-d-11-00262.1) doi: 10.1175/bams-d-11-00262.1
- 247 Ramsdell, J. V., Jr, & Rishel, J. P. (2007, February). *Tornado Climatology of the
 248 Contiguous United States* (Tech. Rep. Nos. NUREG/CR-4461, PNNL-15112).
 249 P.O. Box 999, Richland, WA 99352: Pacific Northwest National Laboratory.
- 250 Romps, D. M. (2011, jan). Response of tropical precipitation to global warm-
 251 ing. *Journal of the Atmospheric Sciences*, *68*(1), 123–138. Retrieved from
 252 <https://doi.org/10.1175/2010jas3542.1> doi: 10.1175/2010jas3542.1
- 253 Seeley, J. T., & Romps, D. M. (2015, nov). Why does tropical convective avail-
 254 able potential energy (cape) increase with warming? *Geophysical Research
 255 Letters*, *42*(23), 10,429-10,437. Retrieved from [https://doi.org/10.1002/
 256 2015GL066199](https://doi.org/10.1002/2015GL066199) doi: 10.1002/2015GL066199
- 257 Singh, M. S., & O’Gorman, P. A. (2013, aug). Influence of entrainment on the ther-
 258 mal stratification in simulations of radiative-convective equilibrium. *Geophysi-
 259 cal Research Letters*, *40*(16), 4398–4403. Retrieved from [https://doi.org/10.
 260 1002/grl.50796](https://doi.org/10.1002/grl.50796) doi: 10.1002/grl.50796
- 261 Sobel, A. H., & Camargo, S. J. (2011, jan). Projected future seasonal changes in
 262 tropical summer climate. *Journal of Climate*, *24*(2), 473–487. Retrieved from
 263 <https://doi.org/10.1175/2010jcli3748.1> doi: 10.1175/2010jcli3748.1
- 264 Thompson, R., & Vescio, M. (1998). The Destruction Potential Index - A Method
 265 for Comparing Tornado Days. In *19th conference on severe local storms*.
- 266 Tippett, M. K., Lepore, C., & Cohen, J. E. (2016, dec). More tornadoes in
 267 the most extreme u.s. tornado outbreaks. *Science*, *354*(6318), 1419–
 268 1423. Retrieved from <https://doi.org/10.1126/science.aah7393> doi:
 269 10.1126/science.aah7393
- 270 Tippett, M. K., Sobel, A. H., Camargo, S. J., & Allen, J. T. (2014). An empirical

271 relation between U.S. tornado activity and monthly environmental parameters.
272 *Journal of Climate*, 27, 2983-2999.
273 Trapp, R. J., Dittenbach, N. S., & Gluhovsky, A. (2009, Jan). Transient response
274 of severe thunderstorm forcing to elevated greenhouse gas concentrations.
275 *Geophysical Research Letters*, 36(1). Retrieved from [http://dx.doi.org/](http://dx.doi.org/10.1029/2008GL036203)
276 10.1029/2008GL036203 doi: 10.1029/2008gl036203